Hindawi
International Journal of Antennas and Propagation
Volume 2022, Article ID 4587930, 12 pages
https://doi.org/10.1155/2022/4587930

Research Article

Analysis of Induced Current on Power Transmission Lines for the Reradiation Interference in Medium Wave Based on Characteristic Modes

Bo Tang,[1,2] Xiaofeng Yang,[1] Jiangong Zhang,[3] Zhibin Zhao,[4] Feng Wang,[1] and Zheyuan Gan[3]

[1]*College of Electrical Engineering & New Energy, China Three Gorges University, Yichang 443002, China*
[2]*Hubei Provincial Engineering Technology Research Center for Power Transmission Line, Yichang 443002, China*
[3]*China Electric Power Research Institute, Wuhan 430073, China*
[4]*College of Electrical and Electronic Engineering, North China Electric Power University, Beijing 100096, China*

Correspondence should be addressed to Xiaofeng Yang; 1079374317@qq.com

Received 13 September 2022; Revised 9 October 2022; Accepted 22 October 2022; Published 11 November 2022

Academic Editor: Ravi Gangwar

The reradiation interference from power transmission lines (PTL) on the adjacent wireless stations is directly caused by the induced current on metal parts, which means the interference could be suppressed by reducing the induced current. In order to effectively analyze the induced current of PTL, a method for analyzing induced current on PTL based on characteristic modes is proposed combining MoM with intrinsic modes. This method breaks through the traditional antenna resonance theory proposed by IEEE and could effectively avoid model equivalent defects and frequency limitations of traditional methods. Firstly, a generalized characteristic equation about the characteristic mode currents of PTL is constructed, and the numerical solutions of the characteristic mode currents are obtained by the idea of a discrete solution. Then, through the weighted orthogonal relationship between different characteristic mode currents, the expansion coefficients of the characteristic mode currents are obtained; finally, combined with the Poynting theorem, the physical meaning of the expansion coefficients and their related quantities are explained from the perspective of energy and the analysis of the induced current is realized from the physical level. The results of the example analysis show that the error between the peak frequencies of the induced current calculated by the method in this paper and the peak frequencies calculated by MoM does not exceed 2.46% and the method in this paper can well explain the disappearance of the "double wavelength loop resonance frequency" under the excitation of a vertically polarized plane wave.

1. Introduction

With the construction of UHV (ultra-high voltage) projects in China, the number of power transmission lines (PTL) as large-scale metal scatterers continues to increase, which inevitably causes serious reradiation interference on adjacent wireless stations [1]. At present, the problem of reradiation interference is mainly solved by determining the projection distance based on the allowable interference threshold value, which obviously needs excessive space distance and cannot deal with the existing interference between PTL and wireless stations which has been built [2]. The research of IEEE shows that the reradiation interference level of PTL is directly related to the induced current on its metal parts [3]. Therefore, the effective analysis of the induced current on PTL and the internal mechanism of its variation can provide a theoretical reference for the active suppression of reradiation interference, which is of great significance to solve the electromagnetic compatibility problem between PTL and wireless stations.

Due to the complex structure and huge size of the PTL, it is difficult to directly measure the induced current.

Therefore, the early research on the induced current of PTL in the medium wave was mainly realized by simulation calculation [4]. The study in [5] summarizes the methods of simulation calculation and proposes a method to solve the induced current of PTL by MoM (method of moments). In this method, the power towers and the ground wires are equivalent to wire antenna models with different radii in different frequency bands, and the conductors could be ignored in the modeling because it is perpendicular to the direction of the excitation electric field. Although these methods of simulation calculation can obtain the numerical value of the induced current on PTL, they cannot reasonably explain the variation of the induced current [6].

Therefore, the follow-up research used the antenna resonance theory in the analysis of induced current on PTL under the excitation of the wire antenna, which is based on the equivalent model of PTL in a medium wave band. According to this theory, the analysis of induced current is divided into two cases: when the power towers are connected to the ground wires, the "loop antenna" could be equivalent to the power towers, the ground wires, and their mirror images to the ground within a span. At this time, the variation of the induced current can be analyzed according to the resonance theory of the loop antenna and then proposes the "integer wavelength loop resonance frequency" corresponding to the peak values of the induced current [3, 7]; when the power towers are insulated from the ground wires, the "loop antenna" is no longer included in the PTL, but the power towers can still be regarded as a wire antenna perpendicular to the ground. Based on this, the "$\lambda/4$ resonance frequency" corresponding to the peak values of the induced current can be obtained by the resonance theory of the half-wave antenna [3, 8]. However, it is obviously not universal to analyze the induced current only under the excitation of wire antennas [9]. Therefore, the study in [10] continued to solve the induced current under the excitation of the vertically polarized plane wave. The result shows that there is no peak value of the induced current corresponding to the "double wavelength loop resonance frequency," and this phenomenon cannot be reasonably explained according to the antenna resonance theory.

In addition, the study in [11] through experiments found that when the frequency reaches the medium wave band above 1.7 MHz, the details of power towers become non-negligible relative to the wavelength of the electromagnetic wave. At this time, the power towers can no longer be simply equivalent to several wire antennas, and the variation of the induced current on PTL can no longer be analyzed according to the antenna resonance theory. Therefore, the follow-up research can only rely on a more refined simulation model and uses MoM to simply solve the induced current in 1.7 MHz–3 MHz, but it is also unable to explain the internal mechanism for the variation of induced current [12].

Considering that the existing methods are difficult to effectively analyze the variation of induced current on PTL for the entire medium wave band, we break through the traditional antenna resonance theory proposed by IEEE and put forward a method for analyzing induced current on PTL based on characteristic modes, which could effectively avoid model equivalent defects and frequency limitations of traditional methods. This method transforms the analysis of induced current on PTL into the analysis of characteristic mode currents and their related quantities and clarifies the physical meaning for the related quantities of characteristic mode currents in combination with the Poynting theorem, which can analyze the internal mechanism for the variation of induced current from the physical level.

2. Induced Current on PTL and Existing Analysis Methods

2.1. Induced Current on PTL. PTLs are mainly composed of conductors, ground wires, insulator strings, line fittings, power towers, tower foundations, and grounding devices. The metal parts exposed above the ground mainly include power towers, conductors, and ground wires [13]. From the view of electromagnetism, the power towers, conductors, and ground wires can be regarded as a collection of countless charged particles. When the incident electromagnetic wave from the wireless stations irradiates the metal parts of PTL, it will interact with the charged particles. With the alternating influence of the incident electromagnetic wave, the metal parts of PTL will generate induced electromotive force, and the induced electromotive force will further cause the charged particles to move and generate alternating induced current.

The alternating induced current will further launch electromagnetic waves into space and generate a new scattered field near PTL, which is the reradiation field. The superposition of the reradiation field and the original incident field changes the magnitude and phase of the original incident field, which causes interference to the signal of wireless stations.

2.2. Existing Analysis Methods for Induced Current. At present, the combination of antenna resonance theory and simulation calculation method is mainly used to analyze the induced current on PTL in the entire medium wave band.

Antenna resonance theory mainly includes loop antenna resonance theory and half-wave antenna resonance theory. When the power towers are connected to the ground wires, the PTL can be equivalent to a "loop antenna" as shown in Figure 1(a). According to the resonance mechanism of the loop antenna, when the length of the "loop antenna" in Figure 1(a) is an integer multiple of the wavelength of an electromagnetic wave, the peak value of the induced current will appear in the loop, and the corresponding frequency of an electromagnetic wave is called "integer wavelength loop resonance frequency." When the power towers are insulated from the ground wires, because the ground wires are perpendicular to the electric field direction of electromagnetic wave, no induced current will be generated. Therefore, it is only necessary to consider the induced current on the power towers. At this time, the PTL can be equivalent to several wire antennas perpendicular to the ground as shown in Figure 1(b). According to the resonance mechanism of the

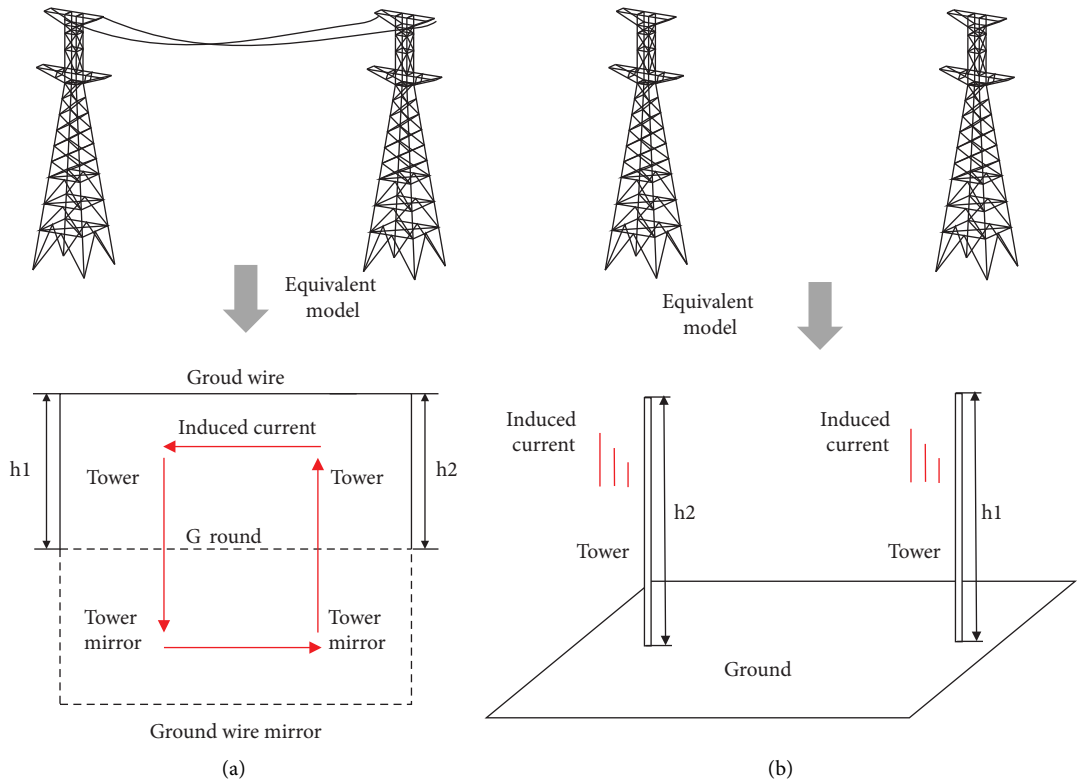

Figure 1: Equivalent models of PTL for one span. (a) The equivalent model of the loop antenna. (b) The equivalent model of wire antenna.

half-wave antenna, when the length of the line antenna in Figure 1(b) is a quarter wavelength of the electromagnetic wave, the peak value of the induced current will appear on the wire antenna, and the corresponding frequency of an electromagnetic wave is called "$\lambda/4$ resonance frequency."

It can be seen that whether the antenna resonance theory is effective for the analysis of the induced current mainly depends on whether the PTL can be equivalent to the loop antenna or the wire antenna. When the frequency reaches the medium wave band above 1.7 MHz, the details of the power towers become nonnegligible relative to the electromagnetic wave wavelength [3]. At this time, a power tower can no longer be simply equivalent to a single-wire antenna, so the antenna resonance theory is no longer applicable. Therefore, the frequency range applicable to the antenna resonance theory is very limited.

In addition, according to the generation and reradiation mechanism of the induced current on PTL in Section 2.1, the PTL are actually passively emitting electromagnetic wave to the outside under the external excitation of electromagnetic waves, which is different from the antenna that actively radiates electromagnetic wave to the outside. Therefore, even if the frequency is below 1.7 MHz, the PTL and the antennas cannot be completely equivalent, which is also the reason why the peak value of the induced current does not appear at the "double wavelength loop resonance frequency" under the excitation of the vertically polarized plane wave. Thus, the applicable conditions of the antenna resonance theory need further verification.

When the frequency reaches above 1.7 MHz because the antenna resonance theory is no longer applicable, only the simulation calculation method can be used to analyze the induced current on PTL. The basic principle of the simulation calculation is to solve the line electric field integral equation for PTL by MoM. According to [14], the line electric field integral equation for PTL is as follows:

$$\mathbf{l}\cdot\mathbf{E}^{\mathrm{i}}(\mathbf{r}) = -j\omega\mu\mathbf{l}\cdot\int_{\mathrm{l}'}\mathbf{l}'g\left(\mathbf{r},\mathbf{r}'(\mathbf{l}')\right)\mathbf{J}'\,\mathrm{d}l' + \frac{1}{j\omega\varepsilon}\frac{\mathrm{d}}{\mathrm{d}l}\int_{\mathrm{l}'}g\left(\mathbf{r},\mathbf{r}'(\mathbf{l}')\right)\frac{\mathrm{d}\mathbf{J}'}{\mathrm{d}l'}\,\mathrm{d}l', \tag{1}$$

where l is the unit vector in the axis direction of the thin wire; $\mathbf{E}^{i}(\mathbf{r})$ is the electric field strength of the incident electromagnetic wave; ω is the angular frequency of incident electromagnetic wave; μ is the magnetic permeability; ε is the dielectric constant; $g(\mathbf{r},\mathbf{r}'(\mathbf{l}'))$ is Green's function; and $\mathbf{J}'$ is the induced current density of the thin wire.

After that, the electric field integral equation in equation (1) can be solved by MoM. First, select the known basis function f_n to discretely expand the induced current to be

solved in equation (1); then, use the appropriate weight function f_m to test the discrete equation (1), and then obtain the matrix equation for the expansion coefficient of the basis function as follows:

$$[\mathbf{Z}]\boldsymbol{\alpha} = \mathbf{b}, \tag{2}$$

where the matrix $[\mathbf{Z}]$ is the impedance matrix obtained after the discretization of (1); $[\mathbf{Z}] = [\langle \mathbf{f}_m, \mathbf{L}(\mathbf{f}_n)\rangle]$ (where $\mathbf{L}$ is a linear symmetric operator, corresponding to the linear transformation process of $\mathbf{J}'$ on the right side of (1); $\langle \mathbf{A}, \mathbf{B}\rangle$ represents the inner product of two vector functions $\mathbf{A}$ and $\mathbf{B}$, whose magnitude is equal to the integral for the product of the two vector functions); $\boldsymbol{\alpha}$ is the column vector formed by the expansion coefficient of the impulse basis function; and $\mathbf{b}$ is the column vector related to the excitation source, $b = [\langle f_m, -\mathbf{E}_\mathbf{i}(\mathbf{r})\rangle]^T$. By solving (2), the induced current on PTL can be obtained.

From the basic principle of simulation calculation, it can be seen that if only this method is used to analyze the induced current on PTL, there will be two obvious drawbacks. First, the induced current solved by the simulation calculation method is closely related to the impedance matrix $[\mathbf{Z}]$ in (2), but the impedance matrix $[\mathbf{Z}]$ is obtained by discretizing the electric field integral equation in equation (1) by MoM. Therefore, the analysis of the induced current by this method always depends on the analysis of the electric field integral equation and can only give a very limited physical explanation for the variation of induced current. Second, the column vector $\mathbf{b}$ on the right side of equation (2) is closely related to the external excitation of PTL. Since the column vector $\mathbf{b}$ obtained under different external excitations is quite different, the induced current obtained by equation (2) is also different. Therefore, the simulation calculation method relies on specific external excitations, so it is almost impossible to provide the inherent variation law of induced current.

3. The Analysis of Induced Current on PTL Based on Characteristic Modes

3.1. The Concept and Application of Characteristic Modes. The characteristic modes refer to the inherent mode responses obtained by the mode decomposition of the total radiation or scattering response for the electromagnetic target [15]. For different solution objects, these inherent mode responses can be embodied as characteristic mode currents or characteristic mode electric fields. According to the theory of characteristic modes, the characteristic modes are quantities irrelevant to the external excitation and only depend on the structural parameters such as the shape and material of the electromagnetic target; but the expansion coefficients after the mode decomposition are quantities related to the external excitation. Obviously, using the characteristic modes can not only study the inherent radiation or scattering characteristics of the electromagnetic target but also analyze the influence of the external excitation on the radiation or scattering response.

According to the analysis in Section 2.1, the induced current generated by the PTL under the excitation of the electromagnetic wave and the reradiation interference generated by it can be attributed to the electromagnetic scattering problems of the electromagnetic target. In addition, existing research shows that under a specific excitation, only a few characteristic modes play a major role in electromagnetic scattering, so the solution to electromagnetic scattering problems can be simplified by only considering the main characteristic modes [16]. According to the above mechanism, we can introduce the characteristic modes into the analysis of the induced current on PTL, study the inherent induced current distribution of PTL by the solution of characteristic mode currents, and analyze the main characteristic mode currents under a specific excitation by the expansion coefficients. From this, the actual variation law of the induced current on PTL can be obtained.

3.2. The Solution of Characteristic Mode Currents for PTL. According to the solution method of characteristic mode currents for the electromagnetic target [17], the generalized characteristic equation in the form of the matrix for PTL is established as follows:

$$[\mathbf{X}][\mathbf{I}]_N = \lambda_N [\mathbf{R}][\mathbf{I}]_N, \tag{3}$$

where $[\mathbf{X}]$ and $[\mathbf{R}]$ are, respectively, the real and imaginary parts of the impedance matrix $[\mathbf{Z}]$; $[\mathbf{I}]_N$ is the column vector composed of basis function expansion coefficients for Nth characteristic mode current on PTL, where $[\mathbf{I}]_N = [I_1, I_2, \cdots, I_n]^T$; and λ_N is the characteristic value of the Nth mode for PTL.

By solving (3), the characteristic values λ_N of each mode for PTL and the column vectors $[\mathbf{I}]_N$ corresponding to λ_N can be obtained. Then, the corresponding characteristic mode current $\vec{\mathbf{J}}_N$ can be obtained by the discrete solution method [18], which is as follows:

$$\vec{\mathbf{J}}_N = \sum_n I_n \mathbf{f}_n, \tag{4}$$

where $\mathbf{f}_n$ is the basis function, and the pulse basis functions are selected for the model of PTL in the medium wave band [19].

From the whole process of solving the characteristic mode currents on PTL, it can be seen that the external excitation is not involved in solving equations (3)–(4). Therefore, the characteristic values and characteristic mode currents of each mode finally solved are independent of the external excitation, which can characterize the inherent characteristics of PTL. In addition, it can be seen from (4) that the characteristic mode currents can represent the distribution of the induced current on PTL, which is expressed by the expansion coefficients I_n of n basis functions. To sum up, the characteristic mode currents are inherent distribution characteristics of the induced current on PTL.

3.3. The Solution of Expansion Coefficients for Characteristic Mode Currents. According to the concept of characteristic modes, the actual induced current on PTL can be expressed as the superposition of characteristic mode currents $\overrightarrow{\mathbf{J}}_N$ ($N = 1, 2, \ldots$); that is, the induced current $\mathbf{J}'$ can be decomposed into one by one component of characteristic mode currents $\overrightarrow{\mathbf{J}}_N$ ($N = 1, 2, \ldots$). Taking the induced current on the angle steel of a power tower as an example, the schematic diagram of its mode decomposition is shown in Figure 2.

Therefore, the actual induced current $\mathbf{J}'$ can be expressed as the characteristic mode currents $\overrightarrow{\mathbf{J}}_N$ ($N = 1, 2, \ldots$) as follows:

$$\mathbf{J}' = \sum_N c_N \overrightarrow{\mathbf{J}}_N, \tag{5}$$

where c_N is the expansion coefficient of the characteristic mode currents, which is called the mode weight coefficient. And the expression for c_N is as follows:

$$c_N = \frac{\langle \overrightarrow{\mathbf{J}}_N, \mathbf{E}^i(\mathbf{r}) \rangle}{1 + j\lambda_N} = \frac{\int_{l'} \overrightarrow{\mathbf{J}}_N \cdot \mathbf{E}^i(\mathbf{r}) dl'}{1 + j\lambda_N}, \tag{6}$$

where the inner product $\int_{l'} \overrightarrow{\mathbf{J}}_N \cdot \mathbf{E}^i(\mathbf{r}) dl'$ in the numerator is the mode excitation coefficient of the Nth mode, which is usually represented by the symbol ME_N, and the denominator can be used to define the mode significance MS_N of the Nth mode. The two coefficients are as follows:

$$\begin{cases} ME_N = \int_{l'} \overrightarrow{\mathbf{J}}_N \cdot \mathbf{E}^i(\mathbf{r}) dl', \\ MS_N = \left| \dfrac{1}{1 + j\lambda_N} \right|. \end{cases} \tag{7}$$

According to (6) and (7), it can be seen that the value of the mode weight coefficient c_N depends on the mode excitation coefficient ME_N and the mode significance MS_N. Only when these two coefficients are both large, the mode weight coefficient can be guaranteed to be large so that the corresponding mode becomes the significant mode that dominates the actual induced current [20]. According to the expression of the mode excitation coefficient ME_N, it can be known that its value depends on the value of the inner product between the external excitation $\mathbf{E}^i(\mathbf{r})$ and the characteristic mode current $\overrightarrow{\mathbf{J}}_N$, that is, the degree of coupling between the two. But the mode significance MS_N is a quantity independent of the external excitation $\mathbf{E}^i(\mathbf{r})$, and its value is only related to the characteristic value λ_N.

3.4. Physical Meaning of Characteristic Mode Current-Related Quantities. The actual induced current on PTL is decomposed mathematically in Sections 3.2 and 3.3 but does not explain the physical meaning for the related quantities of characteristic mode current. Therefore, this section will combine the Poynting theorem to deeply analyze the physical meaning of the related quantities of characteristic mode current from the perspective of energy.

As shown in Figure 3, there is a PTL in the volume V contained by the closed surface S_∞. It is assumed to be the Nth-order characteristic mode current $\overrightarrow{\mathbf{J}}_N$ existing on the surface S of the PTL, and the corresponding $\mathbf{E}_N$ and $\mathbf{H}_N$ are, respectively, the Nth-order characteristic mode electric field and the magnetic field generated by $\overrightarrow{\mathbf{J}}_N$. ε_0 and μ_0 are the permittivity and permeability in volume V, and $\overrightarrow{n}$ is the outward normal unit vector of S_∞.

Applying the Poynting theorem in the volume V yields the following relationship of energy:

$$-\iint_S \mathbf{E}_N \cdot \overrightarrow{\mathbf{J}}_N^* dS = \iint_{S\infty} (\mathbf{E}_N \times \mathbf{H}_N^*) \cdot \overrightarrow{n} dS + j\omega \iiint_V \left(\mu_0 |\mathbf{H}_N|^2 - \varepsilon_0 |\mathbf{E}_N|^2 \right) \mathrm{d}V, \tag{8}$$

where the left side of the equation represents the total power provided by the characteristic mode current $\overrightarrow{\mathbf{J}}_N$ for the entire system; the first item on the right side of the equation represents the energy radiated to S_∞, indicating the far-field radiated power, which is active power; the second item on the right side of the equation represents the storage power of energy in volume V, which is reactive power.

Assuming that the metal part of the PTL is an ideal conductor, according to the boundary conditions of the ideal conductor surface, the relationship between the characteristic mode current and electric field can be obtained as follows:

$$\mathbf{E}_N = -\mathbf{L}\left(\overrightarrow{\mathbf{J}}_N \right). \tag{9}$$

Substituting (9) into (8) and discretizing the characteristic mode current $\overrightarrow{\mathbf{J}}_N$ according to (4), we can obtain the following:

$$-\iint_S \mathbf{E}_N \cdot \overrightarrow{\mathbf{J}}_N^* dS = \iint_S \mathbf{L}\left(\overrightarrow{\mathbf{J}}_N \right) \cdot \overrightarrow{\mathbf{J}}_N^* dS = \langle \overrightarrow{\mathbf{J}}_N^*, \mathbf{L}\left(\overrightarrow{\mathbf{J}}_N \right) \rangle = [\mathbf{I}]_\mathbf{N}^\mathbf{H} \cdot [\mathbf{Z}] \cdot [\mathbf{I}]_N, \tag{10}$$

where $[\cdot]^H$ means to take the conjugate transpose.

Substitute $[\mathbf{Z}] = [\mathbf{R}] + j[\mathbf{X}]$ into equation (10) to get the following:

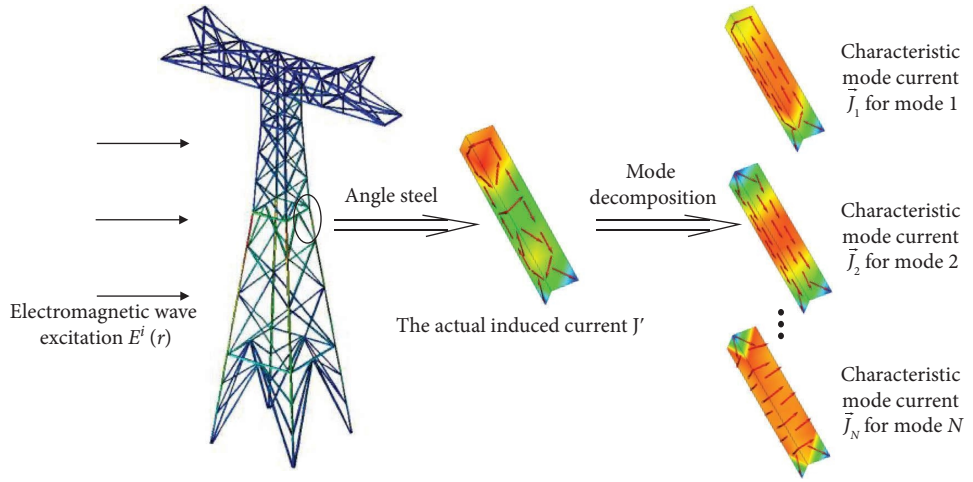

Figure 2: Schematic diagram for the mode decomposition of the induced current on PTL.

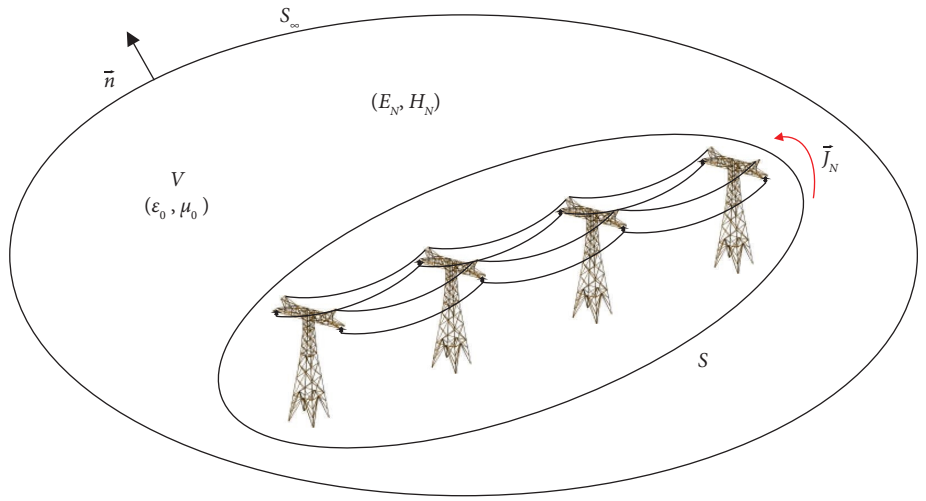

Figure 3: Schematic diagram of the N th-order characteristic mode current and field for the PTL.

$$-\iint_S \mathbf{E}_N \cdot \vec{\mathbf{J}}_N^* dS = [\mathbf{I}]_N^H \cdot [\mathbf{R}] \cdot [\mathbf{I}]_N + j[\mathbf{I}]_\mathbf{N}^\mathbf{H} \cdot [\mathbf{X}] \cdot [\mathbf{I}]_N. \tag{11}$$

Simultaneous (8) and (11) can obtain the following correspondence:

$$\begin{cases} [\mathbf{I}]_N^H \cdot [\mathbf{R}] \cdot [\mathbf{I}]_N = \oiint_{S_\infty} (\mathbf{E}_N \times \mathbf{H}_N^*) \cdot \vec{n} dS, \\ [\mathbf{I}]_N^H \cdot [\mathbf{X}] \cdot [\mathbf{I}]_N = \omega \iiint_V \left(\mu_0 |\mathbf{H}_N|^2 - \varepsilon_0 |\mathbf{E}_N|^2\right) dV. \end{cases} \tag{12}$$

It can be seen from (12) that $[\mathbf{I}]_\mathbf{N}^\mathbf{H} \cdot [\mathbf{R}] \cdot [\mathbf{I}]_N$ represents the far-field radiated power for the system in Figure 3, and $[\mathbf{I}]_\mathbf{N}^\mathbf{H} \cdot [\mathbf{X}] \cdot [\mathbf{I}]_N$ represents the storage power of energy for the system.

According to the weighted orthogonality of the characteristic mode currents [16] and combined with (4), we can get the following:

$$[\mathbf{I}]_\mathbf{N}^\mathbf{T} [\mathbf{X}] [\mathbf{I}]_N = \lambda_N. \tag{13}$$

Because (3) is the generalized characteristic equation of real symmetric matrices [18], $[\mathbf{I}]_N$ to be solved must be a vector composed of real numbers, then $[\mathbf{I}]_\mathbf{N}^\mathbf{H} = [\mathbf{I}]_\mathbf{N}^\mathbf{T}$. Considering the above relationship and further combining (12) and (13), we can obtain the following:

$$\lambda_N = \omega \iiint_V \left(\mu_0 |\mathbf{H}_N|^2 - \varepsilon_0 |\mathbf{E}_N|^2\right) dV. \tag{14}$$

It can be seen from (14) that the characteristic value represents the storage power of energy in the N th mode. When the characteristic value at a certain frequency is 0, it means that the storage power of energy in this mode is 0. At this time, the radiation power reaches the maximum value, the mode is in the resonance state, and the corresponding characteristic mode current will reach the peak value. Since the characteristic value is independent of external

excitation, according to the variation of the characteristic value with the frequency, the internal resonance frequencies corresponding to the peak values of the characteristic mode current can be screened out. Because the mode significance is only related to the characteristic value, the internal resonant frequencies can also be screened out by the mode significance. It can be seen from (7) that when the characteristic value tends to 0 at a certain frequency, the mode significance tends to be 1, and the corresponding mode is in the resonance state.

However, in the actual case of external excitation, not all the peak values of the induced current corresponding to the resonant modes (there is a mode of $\lambda_N = 0$ or $MS_N = 1$ in the research band) can be shown, and only the peak values of the induced current corresponding to the significant modes with larger mode weight coefficients can be shown. This requires a better coupling degree between the characteristic mode current and the external excitation, ensuring that the mode excitation coefficient of the resonant mode is larger, and then the mode weight coefficient is also larger.

4. Induced Currents and Its Mode Decomposition of PTL in the Medium Wave Band

4.1. The Establishment of Models. When the frequency is below 1.7 MHz, the relevant modeling and calculation are carried out using the V1S tower for the 500 kV double-circuit PTL proposed by IEEE as an example. Since the cross-sectional size of the power tower is small compared to the wavelength of electromagnetic waves below 1.7 MHz, the structural details of the power tower can be ignored, and the power tower is directly equivalent to a single-line model. According to [3, 5], the power tower in the medium wave band is equivalent to a line model with a radius of 3.51 m, and the ground wire is equivalent to a line model with a radius of 0.71 m. The final simulation model is shown in Figure 4.

Considering that the smallest unit that constitutes a PTL is two adjacent power towers within a span and the ground wire connecting the power towers. Therefore, the study in [6] only calculated the induced current on the PTL within the representative span and found that the calculated result of the induced current was in good agreement with the measured result. For this reason, this paper also simplifies the simulation model in Figure 4 and only considers the PTL within a representative span in the subsequent calculation of the induced current.

Because the calculation example of IEEE does not involve the analysis of the induced current on PTL above 1.7 MHz, this paper will carry out the related modeling and calculation in 1.7 MHz–3 MHz according to the tower type in the calculation example of [21]. In this example, the ZP30101 tower of the ±800 kV Xiangjiaba-Shanghai UHVDC PTL is used. According to the actual size of the ZP30101 tower, a PTL model considering the space truss structure of the power tower is established. The final simulation model is shown in Figure 5.

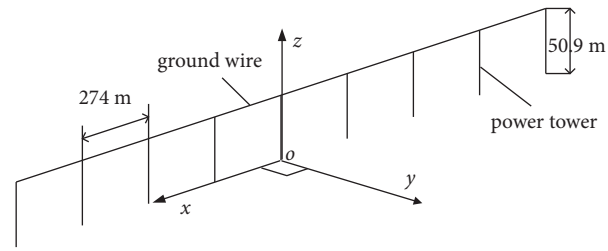

Figure 4: Model for calculation of induced current on PTL below 1.7 MHz.

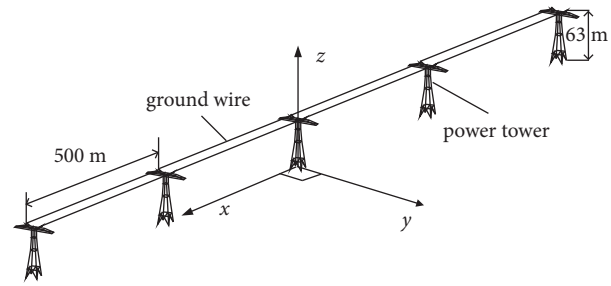

Figure 5: Model for calculation of induced current on PTL in 1.7 MHz–3 MHz.

In order to simplify the calculation, when analyzing the induced current on PTL in this frequency band, the same simplified processing method is also adopted as in reference [6] and only the PTL within the representative span is considered.

After the model is established, it is necessary to set the excitation to solve and analyze the actual induced current. Due to the different types, sizes, and models of transmitting antennas for various wireless stations, the magnitude and distribution of the induced current on PTL will be different, so the specific station antenna cannot be used to stimulate the induced current. Therefore, it can only be assumed that various wireless stations emit electromagnetic waves at infinity to stimulate the induced current. Since the power tower is perpendicular to the ground, consider the most serious interference situation for the wireless stations, that is, using a vertically polarized plane wave for external excitation.

4.2. Analysis of Induced Current on PTL below 1.7 MHz. The analysis of induced current by characteristic modes below 1.7 MHz is carried out using the simulation model in Figure 4, and the line segment length of the simulation model is 10 m. Because the range of the medium wave band starts from 0.3 MHz, the frequency range of the electromagnetic wave is set to 0.3~1.7 MHz, and the value of the frequency step is 25 kHz.

According to the simulation model, the generalized characteristic equation of PTL as shown in (3) is constructed, and the generalized characteristic equation at each frequency point is solved to obtain the characteristic values for each mode. Substitute the characteristic values into (7) to further obtain the mode significances for each mode. And

the variation of the mode significance for each mode with frequency is shown in Figure 6(a).

It can be seen from Figure 6(a) that in the research frequency band, only mode 1, mode 3, and mode 4 are resonant modes, and the internal resonance frequencies corresponding to the peak values of the characteristic mode currents for each mode are respectively 0.47 MHz, 0.91 MHz, and 1.29 MHz. But the peak value of the mode significance for mode 2 in the entire research frequency band is 0.458, which is far from meeting the requirements of mode resonance. Therefore, mode 2 cannot be a significant mode that controls the actual induced current in this research frequency band.

According to the loop antenna resonance theory in the IEEE calculation example, when the frequency of the electromagnetic wave reaches the "integer wavelength loop resonance frequency," the induced current on PTL will have a peak value [3]. According to the geometric parameters of the simulation model in Figure 4, it can be known that the length of the corresponding "loop" is 751.6 m, and the resonant frequencies of the 1, 2, and 3 times wavelength loops are respectively 0.43 MHz, 0.86 MHz, and 1.29 MHz This is basically consistent with the calculation result in Figure 6, so it can be considered that the calculation results in Figure 6 are accurate.

From the analysis in the last two paragraphs of Section 3.4, whether the peak values of the characteristic mode currents in Figure 6(a) can be expressed under the condition of external excitation, in addition to satisfying the conditions for resonance in the research frequency band, the corresponding modes also need to have a good energy coupling relationship with the external excitation at the internal resonant frequencies. According to Section 4.1, the external excitation to the simulation model adopts a vertically polarized plane wave of 1 V/m, and the incident direction of it is perpendicular to the direction of the PTL. Then, the variation of the mode excitation coefficient with frequency for each mode is obtained by (7), which is shown in Figure 6(b).

It can be seen from Figure 6(b) that the mode excitation coefficients of mode 1 and mode 4 at their respective internal resonant frequencies are large, which are respectively 47.97 and 15.72, indicating that the energy coupling between the external excitation and the characteristic mode currents of mode 1 and mode 4 is better. However, the mode excitation coefficient of mode 3 is 0 at its internal resonant frequency. According to (7), the mode excitation coefficients depend on the inner product of the external excitation and the characteristic mode currents. Because the magnitude and direction of the external excitation are known, the magnitude and direction of the characteristic mode currents also need to be given to further explain the above phenomenon.

According to (3), the distributions of the characteristic mode currents at the resonant frequencies are calculated, and they are shown in Figure 7. It should be noted that mode 2 is not a resonant mode, so there is no need to study the characteristic mode current of this mode.

From Figure 7, we can see that the characteristic mode current on the PTL includes 3 parts, which are the current on the ground wire, on the left tower, and on the right tower. Therefore, the energy coupling between the characteristic mode current and the external excitation also includes 3 parts. Taking mode 3 as an example, because the external excitation is perpendicular to the direction of the ground wire, the energy coupling between the characteristic mode current on the ground wire and the external excitation is 0. And it can be seen from Figure 8 that the characteristic mode current of mode 3 on the left tower and the characteristic mode current on the right tower are 180 degrees out of phase, but the phase of the external excitation incident on the 2 power towers is same. This results in the total energy coupling between the characteristic mode currents on the 2 towers and the external excitation being 0. Finally, the total energy coupling after the superposition of the 3 parts is also 0, that is, the mode excitation coefficient of mode 3 is 0. As a result, even if mode 3 is a resonant mode in the research frequency band, the peak value corresponding to the characteristic mode current of mode 3 will not appear.

At last, it is necessary to comprehensively consider the mode excitation coefficients and mode significances of each mode to determine the significant modes in the research frequency band. Substitute these two coefficients into (6) to obtain the mode weight coefficients of each mode, and the calculation results are shown in Figure 8(a). The induced current on PTL calculated by MoM is shown in Figure 8(b). The simulation model of MoM also uses the single-line model in Figure 4, and the relevant calculations are achieved by FEKO 2021.

It can be seen from Figure 8(a) that only the mode weight coefficient of mode 1 is the largest in the 0.3~0.92 MHz, so mode 1 is a significant mode that mainly controls the actual induced current in this frequency range. Therefore, the internal resonant frequency of mode 1 and the corresponding peak value of the induced current can be displayed. Similarly, in 0.92 MHz~1.7 MHz, the mode weight coefficient of mode 4 is the largest, so the internal resonant frequency of mode 4 and the corresponding peak value of the induced current can be displayed. However, the mode weight coefficients of mode 2 and mode 3 in the entire research frequency band are almost always 0, so the peak value of the induced current corresponding to these two modes will not appear in the entire research frequency band.

In addition, it can be seen from Figure 8(b) that the induced current calculated by MoM has peak values at 0.47 MHz and 1.28 MHz, respectively corresponding to "1 time the wavelength of the loop resonance frequency" and "3 times the wavelength of the loop resonance frequency," and this result is consistent with reference [10]. By comparing Figures 8(a) and 8(b), it can be seen that the frequency of the peak values of the induced current calculated according to the characteristic modes is in good agreement with the calculation result of MoM, and the maximum deviation of frequencies calculated by the two is 0.78%. And the method of characteristic modes can well explain the reason for the disappearance of the peak value of the induced current corresponding to the "2 times the wavelength loop resonance frequency," which makes up for the defects of the antenna resonance theory in analyzing the induced current.

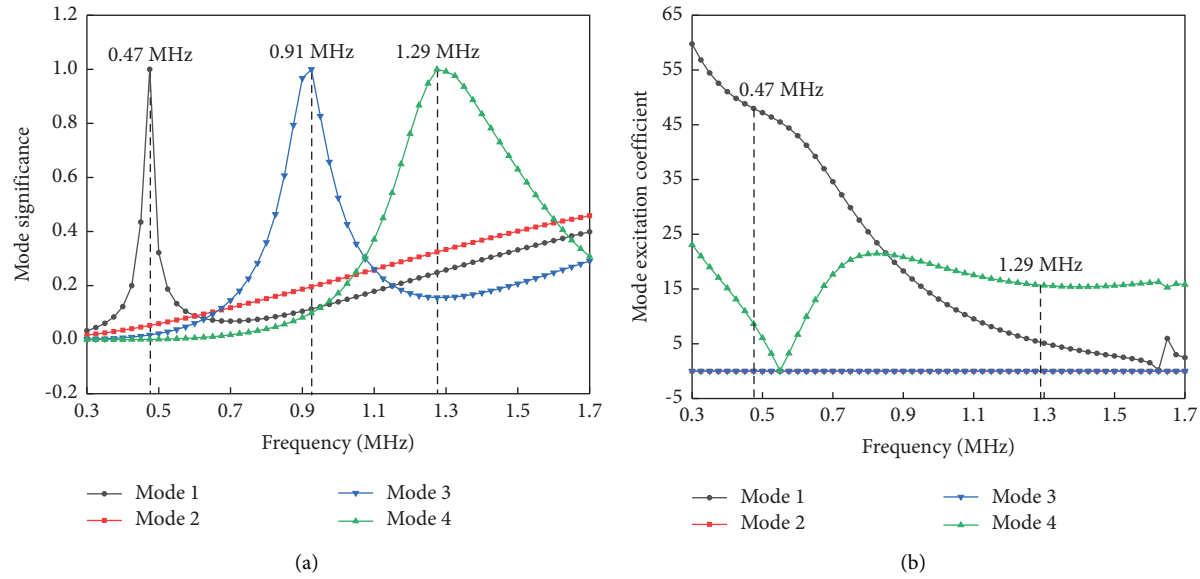

Figure 6: Variation with the frequency of mode significances and mode excitation coefficients. (a) Mode significances. (b) Mode excitation coefficients.

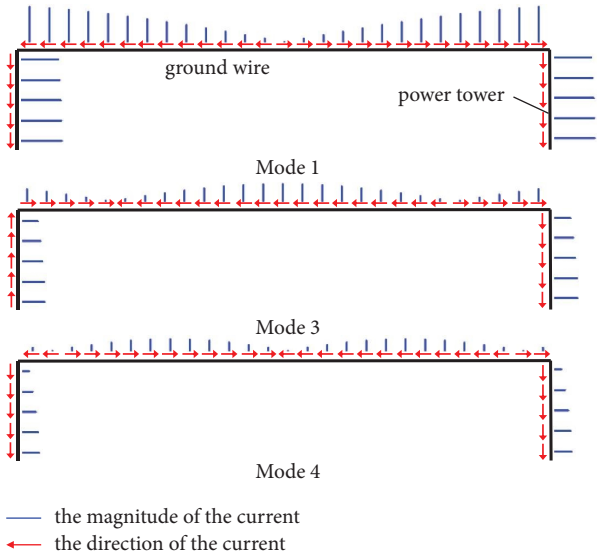

Figure 7: The distribution of characteristic mode current for resonant modes on the PTL. Note: the length of the blue line represents the magnitude of the current at the wire segments, and the currents of the resonant modes use the same normalization method.

4.3. Analysis of Induced Current on PTL in 1.7 MHz–3 MHz. When the frequency is above 1.7 MHz, the model in Figure 5 should be used to analyze and calculate the induced current. Since the upper limit of the medium wave band is 3 MHz, the frequency range of the electromagnetic wave is 1.7~3 MHz, and the frequency step is also 25 kHz. Using the same calculation process as in Section 4.2, the variation with frequency of the mode significance of each mode is obtained as shown in Figure 9(a).

It can be seen from Figure 9(a) that the peak values of the mode significance for 4 modes are both 1 in 1.7~3 MHz, so all 4 modes can reach the resonance state, that is, these 4 modes are all resonant modes in the research frequency band. In addition, it can also be seen that the internal resonance frequencies corresponding to the peak values of the characteristic mode currents are respectively 1.85 MHz, 2.14 MHz, 2.41 MHz, and 2.59 MHz.

In order to further study the coupling between the external excitation and each characteristic mode current in 1.7~3 MHz, continue to use (7) to obtain the mode excitation coefficients of each mode. The calculation results are shown in Figure 9(b).

It can be seen from Figure 9(b) that the mode excitation coefficients of mode 2 and mode 4 at their respective internal resonant frequencies are large, which are respectively 3.57 and 1.4, indicating that the energy coupling between the external excitation and the characteristic mode currents of mode 1 and mode 4 is better. The mode excitation coefficients of mode 1 and mode 3 at their internal resonant frequencies are respectively 0.022 and 0.013 which are completely negligible compared with the mode excitation coefficients of mode 2 and mode 4, indicating that there is almost no energy coupling between the characteristic mode currents of mode 1 and mode 3 and the external excitation.

Finally, in order to judge the significant modes in 1.7~3 MHz, it is also necessary to calculate the mode weight coefficient of each mode according to (6), and the calculation results are shown in Figure 10(a). The induced current calculated by MoM is shown in Figure 10(b). The simulation model of MoM also uses the model in Figure 5, and the relevant calculations are achieved by FEKO 2021.

It can be seen from Figure 10(a) that the mode weight coefficient of mode 2 is the largest at 1.7 MHz~2.66 MHz, so mode 2 is a significant mode in this frequency range, and the peak value of the characteristic mode current corresponding to mode 2 can be displayed near its internal

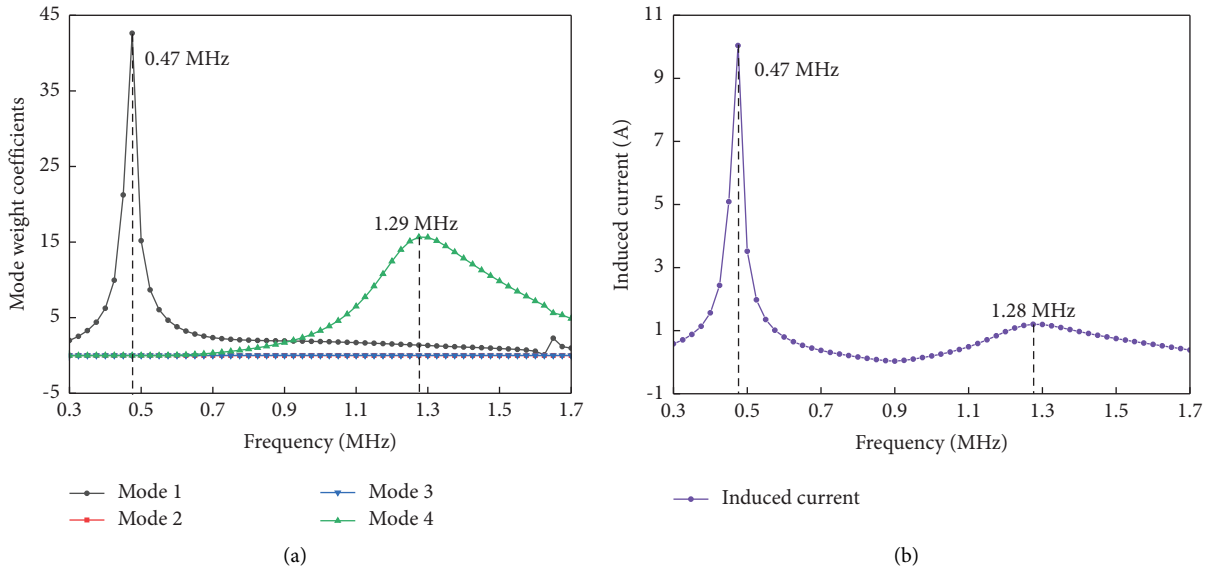

Figure 8: Variation with the frequency of mode weight coefficient and the induced current calculated by MoM. (a) Mode weight coefficients. (b) The induced current calculated by MoM.

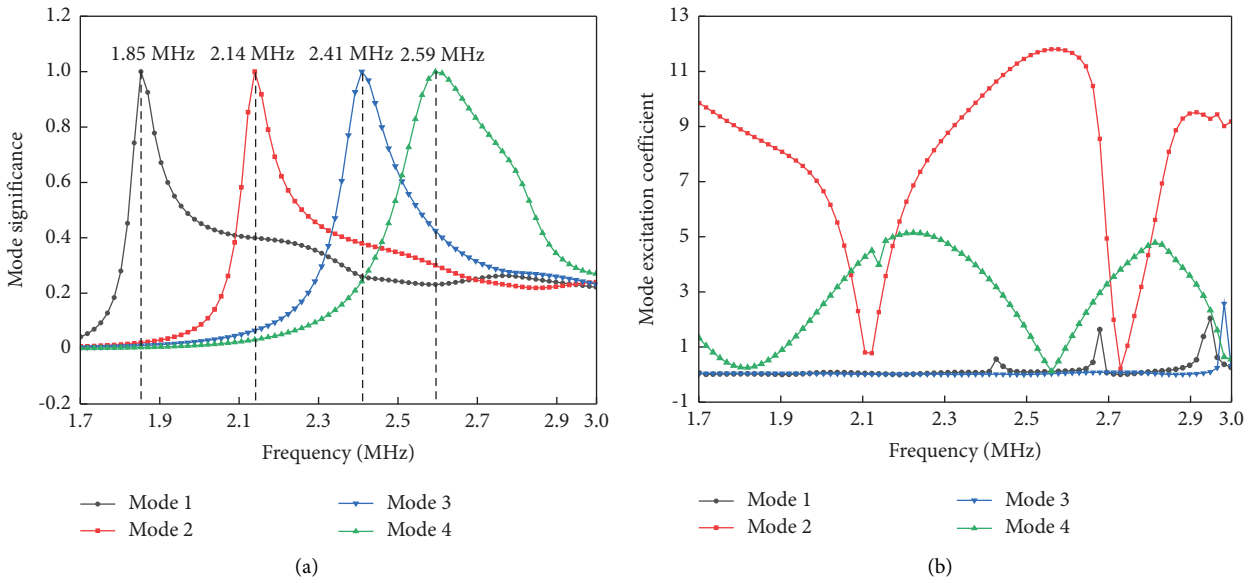

Figure 9: Variation with the frequency of mode significances and mode excitation coefficients. (a) Mode significances. (b) Mode excitation coefficients.

resonant frequency. However, in mode 2, in addition to the peak value near its internal resonant frequency of 2.14 MHz, there is also a peak value near 2.48 MHz. This is because the mode excitation coefficient of mode 2 is close to the peak value near 2.48 MHz, and there is a strong energy coupling between the characteristic mode current of mode 2 and the external excitation. Even if the mode significance is not 1 at 2.48 MHz, under the action of the mode excitation coefficient, the induced current peak value also appears at this frequency point. Similarly, in 2.66 MHz~2.85 MHz, the mode weight coefficient of mode 4 is the largest, so the peak value of the characteristic mode current corresponding to mode 4 can be displayed near its internal resonant frequency. In 2.78 MHz~3 MHz, mode 2 is also a significant mode, but the internal resonant frequency of mode 2 is not in this frequency range, and the energy coupling between the characteristic mode current of mode 2 and the external excitation is also not strong so that there will be no peak value of induced current in this frequency range.

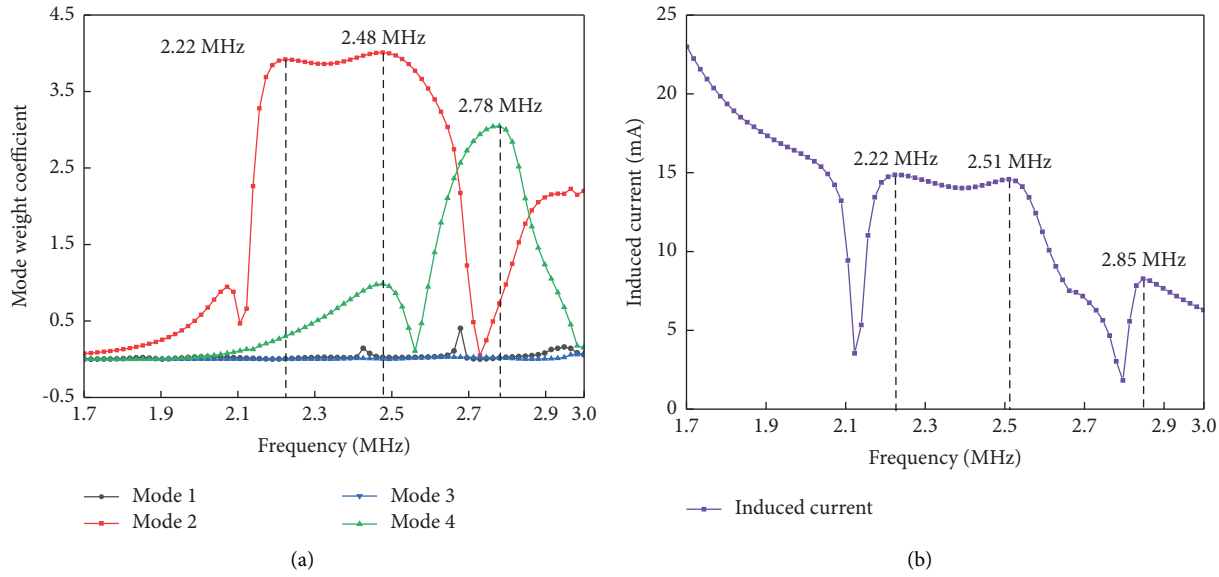

Figure 10: Variation with the frequency of mode weight coefficients and the induced current calculated by MoM. (a) Mode weight coefficients. (b) The induced current calculated by MoM.

In addition, it can be seen from Figure 10(b) that the induced current calculated by MoM has peak values at 2.22 MHz, 2.51 MHz, and 2.85 MHz. By comparing Figures 10(a) and 10(b), it can be seen that the frequency of the peak values calculated by characteristic modes is in good agreement with the calculation result of MoM, and the maximum deviation of the two methods for calculated frequencies is 2.46%. However, the mode weight coefficient of mode 2 at 2.22 MHz in Figure 10(a) is slightly lower than that at 2.48 MHz, while the induced current at 2.22 MHz in Figure 10(b) is slightly higher than that at 2.51 MHz. This is because although the mode weight coefficient at 2.22 MHz is small, the mode significance at this frequency point is much larger than that at 2.48 MHz. Combining the physical meaning of mode significance in Section 3.4, it can be seen that the radiation power of characteristic mode current for mode 2 is the largest at 2.22 MHz, so the final solution of induced current at 2.22 MHz is slightly higher than that at 2.51 MHz.

5. Conclusions

When analyzing the induced current on PTL, the traditional method relies too much on the equivalent relationship between the PTL and the antennas and does not fully consider the preconditions and application scope of the equivalence, resulting in the limitation of the induced current analysis. Therefore, based on the reradiation mechanism of induced current on PTL, this paper introduces the characteristic modes into the analysis of the induced current and clarifies the physical meaning for the related quantities of characteristic mode currents in combination with the Poynting theorem. As a result, an analysis method based on characteristic modes for the induced current on PTL is proposed.

The analysis method of characteristic modes is used to calculate the induced current on PTL in the entire medium wave band, and the results show that the error between the frequency corresponding to the peak values of the induced current calculated by characteristic modes and the frequency calculated by MoM does not exceed 2.46%. In addition, the method in this paper reasonably explains the reason for the disappearance of the "2-wavelength loop resonant frequency" under the excitation of the vertically polarized plane wave from the perspective of energy and the variation mechanism of the induced current in 1.7 MHz–3 MHz, which effectively solves the disadvantages of the antenna resonance theory.

Data Availability

The simulation data used to support the findings of this study are available from the corresponding author upon reasonable request.

Conflicts of Interest

The authors declare that they have no conflicts of interest.

Acknowledgments

This work was supported by Joint Funds of the National Natural Science Foundation of China under grant no. U20A20305.

References

[1] K. G. Balmain and J. S. Belrose, "The effects of reradiation from highrise buildings, transmission lines, towers, and other structures upon AM broadcasting directional arrays," Interim

Report No.2, DOC Project 4-284-15010, Ottawa, Canada, 1978.

[2] J. Zhang, J. Yang, B. Tang, B. Hao, and G. Zheyuan, "Protecting distance between radar stations and UHV power transmission lines," *The Open Electrical & Electronic Engineering Journal*, vol. 12, no. 1, pp. 12–20, 2018.

[3] "IEEE Guide on the Prediction, Measurement, and Analysis of AM Broadcast Reradiation by Power Lines," *IEEE Std. 1260-1996*, 1996.

[4] J. S. Belrose, W. Lavrench, and J. G. Dunn, *The Effects of Reradiation from Highrise Buildings and Transmission Lines upon the Radiation Pattern of MF Broadcasting Antenna Arrays*, Proceedings of AGARD/EPP Meeting, Spatind, Norway, 1979.

[5] C. W. Trueman and S. J. Kubina, "Numerical computation of the reradiation from power lines at mf frequencies," *IEEE Transactions on Broadcasting*, vol. BC-27, no. 2, pp. 39–45, 1981.

[6] C. W. Trueman, S. J. Kubina, and J. S. Belrose, "Corrective measures for minimizing the interaction of power lines with MF broadcast antennas," *IEEE Transactions on Electromagnetic Compatibility*, vol. 25, no. 3, pp. 329–339, 1983.

[7] C. W. Trueman and S. J. Kubina, "Initial assessment of reradiation from power lines," *IEEE Transactions on Broadcasting*, vol. 31, no. 3, pp. 51–65, 1985.

[8] M. A. Tilston and K. G. Balmain, "Medium frequency reradiation from a steel tower power line with and without a detuner," *IEEE Transactions on Broadcasting*, vol. 31, no. 1, pp. 17–26, 1984.

[9] X. Zhang, J. Tang, H. Zhang, and L. Xing-fa, "Reradiation Interference Computation Model of High Voltage Transmission Line to the Shortwave Radio Direction Finding Station," in *Proceedings of the 20th International Zurich Symposium on Electromagnetic Compatibility*, pp. 309–312, IEEE Electromagnetic Compatibility, Zurich, Switzerland, June 2009.

[10] Bo Tang, Y. Wen, X. Zhang et al., "Key problems of solving reradiation interference protecting distance between power transmission line and radio station at MF and SF," *Proceedings of the CSEE*, vol. 31, no. 19, pp. 129–137, 2011.

[11] X. Wu, B. Wan, X. Zhang et al., *Research on the Influence and protection of 1000kV UHV AC Double-Circuit Line in the Same tower on Radio Stations*, China Electric Power Research Institute, Beijing, China, 2008.

[12] T. Bo, W. Yuanfang, Z. Zhibin, and Z. Xiaowu, "Computation model of the reradiation interference protecting distance between radio station and UHV power lines," *IEEE Transactions on Power Delivery*, vol. 26, no. 2, pp. 1092–1100, 2011.

[13] J. Gao and G. Lu, "CRLH transmission lines for telecommunications: fast and effective modeling," *International Journal of Antennas and Propagation*, vol. 2017, pp. 1–5, 2017.

[14] Z. Zhao, Z. Gan, X. Zhang et al., "Passive interference to radio station caused by UHV AC transmission line in shortwave frequency," *High Voltage Engineering*, vol. 35, no. 8, pp. 1818–1823, 2009.

[15] S. Huang, J. Pan, and Y. Luo, "Study on the relationships between eigenmodes, natural modes, and characteristic modes of perfectly electric conducting bodies," *International Journal of Antennas and Propagation*, vol. 2018, Article ID 8735635, 13 pages, 2018.

[16] C. Wang, Y. Chen, and S. Yang, "Application of characteristic mode theory in HF band aircraft-integrated multi-antenna system designs," *IEEE Transactions on Antennas and Propagation*, vol. 67, no. 1, pp. 513–521, 2019.

[17] L. Guo, Y. Chen, and S. Yang, "Generalized characteristic mode formulation for composite structures with arbitrarily metallic-dielectric combinations," *IEEE Transactions on Antennas and Propagation*, vol. 66, no. 7, pp. 3556–3566, 2018.

[18] R. Harrington and J. Mautz, "Computation of characteristic modes for conducting bodies," *IEEE Transactions on Antennas and Propagation*, vol. 19, no. 5, pp. 629–639, 1971.

[19] A. I. Mackenzie, S. M. Rao, and M. E. Baginski, "Method of moments solution of electromagnetic scattering problems involving arbitrarily-shaped conducting/dielectric bodies using triangular patches and pulse basis functions," *IEEE Transactions on Antennas and Propagation*, vol. 58, no. 2, pp. 488–493, 2010.

[20] C. Wang, Y. Chen, G. Liu, and S. Yang, "Aircraft integrated VHF band antenna array designs using characteristic modes," *IEEE Transactions on Antennas and Propagation*, vol. 68, no. 11, pp. 7358–7369, 2020.

[21] Bo Tang, B. Chen, and Z. Zhao, "Frequency estimation of medium-wave reradiation interference resonance from transmission lines based on generalized resonance theory," *Journal of Electrical Engineering & Technology*, vol. 10, no. 3, pp. 1144–1153, 2015.